

SPHERICAL CLUSTERING IN DETECTION OF GROUPS OF CONCOMITANT EXTREMES

V. FOMICHOV AND J. IVANOV

ABSTRACT. There is growing empirical evidence that spherical k -means clustering performs well at identifying groups of concomitant extremes in high dimensions, thereby leading to sparse models. We provide one of the first theoretical results supporting this approach, but also demonstrate some pitfalls. Furthermore, we show that an alternative cost function may be more appropriate for identifying concomitant extremes, and it results in a novel spherical k -principal-components clustering algorithm. Our main result establishes a broadly satisfied sufficient condition guaranteeing the success of this method, albeit in a rather basic setting. Finally, we illustrate in simulations that k -principal-components outperforms k -means in the difficult case of weak asymptotic dependence within the groups.

1. INTRODUCTION

Statistical analysis of high-dimensional data typically relies on various sparsity assumptions, unless structural domain knowledge is available. In the study of extremes, sparsity is especially important since the number of extreme observations is small by definition. The recent survey of [Engelke and Ivanovs \(2021\)](#) reviews different notions of sparsity and the available tools in the context of extreme value statistics. Fundamental here is the notion of concomitant extremes ([Chautru, 2015](#); [Goix et al., 2016](#)), where the focus is on the groups of variables which can be large simultaneously while others are small. Importantly, extremal dependence can be modelled separately in these groups and then combined into a mixture model, thereby leading to dimension reduction.

Mathematically speaking, our interest is in the identification of the lower dimensional faces of \mathbb{R}_+^d charged with mass by the so-called exponent measure. Alternatively, we may look at the faces of the positive simplex charged with mass by the angular (spectral) probability measure. This task, however, is highly non-trivial since only approximate angles coming from a pre-limit distribution, which normally also puts mass on the interior of the simplex, can be obtained in practice.

Various approaches to identification of concomitant extremes and respective maximal sets have been explored in the literature, see [Goix et al. \(2016, 2017\)](#); [Simpson et al. \(2020\)](#); [Chiapino et al. \(2020\)](#); [Meyer and Wintenberger \(2021\)](#); [Jalalzai and Leluc \(2020\)](#). One of the basic ideas is to use a certain neighbourhood of a given face and to assign the respective mass to this face. The simplest method ([Goix et al., 2016](#)) amounts to thresholding the entries of the rescaled extreme observations. Such thresholding, however, often produces a large number of faces with few corresponding observations, see the discussion in [Goix et al. \(2017\)](#) and a numerical illustration in Figure 5 below. Certain grouping of faces is then necessary, see [Chiapino et al. \(2020\)](#).

Key words and phrases. Angular measure; concomitant extremes; dimension reduction; principal components; spherical clustering.

A different approach was proposed by [Chautru \(2015\)](#), and it amounts (ignoring a preliminary dimension reduction step) to spherical k -means clustering ([Dhillon and Modha, 2001](#)) of the approximate angles. Consistency of spherical clustering for a general cost function has been recently established by [Janssen and Wan \(2020\)](#), who also advocated interpreting centroids as ‘prototypes of extremal dependence’. Each centroid, or cluster, can then be attributed to a certain face. One way of doing this is to use thresholding to define respective faces, which has been employed in the review of [Engelke and Ivanovs \(2021\)](#) to obtain interpretable results for a real world 68-dimensional dataset. Importantly, this method can be seen as a *reverse threshold-and-group approach*. Finally, our problem is very different from those addressed by subspace clustering techniques for high-dimensional data ([Gan et al., 2007](#), Ch. 15), which are popular in computer science.

Clustering in detection of concomitant extremes and prototypes of extremal dependence may seem intuitive to some extent, and there is growing empirical evidence in support of this method. The drawback is that there is no theoretical justification, apart from the consistency result by [Janssen and Wan \(2020\)](#). Building upon this result, we provide some basic theory showing that the spherical clustering procedure must indeed work in certain cases. However, we also identify some pitfalls and show that an alternative cost function may be more appropriate for identification of concomitant extremes. It results in a novel *spherical k -principal-components (k -pc) clustering* algorithm (a similar approach in a different context was considered in the empirical study of [Hill et al. \(2013\)](#); see Remark 3.2 below). The name derives from the fact that the Perron–Frobenius eigenvectors of certain non-negative definite matrices with non-negative entries are used instead of the means in the updates of the algorithm. Interestingly, these matrices are the analogues of the cross-moment matrices used by [Cooley and Thibaud \(2019\)](#) and [Drees and Sabourin \(2021\)](#) in their principal component analysis of extremal dependence, whereas the bivariate case has been considered by [Larsson and Resnick \(2012\)](#) in a different context.

Our main results, Theorem 4.2 and Theorem 5.2, provide sufficient conditions guaranteeing the success of clustering in detection of concomitant extremes, albeit in a rather basic setting, when the corresponding groups of coordinates are disjoint. Importantly, k -means fails in some fundamental cases, whereas k -pc is much more robust. Our counterexamples provide further intuition about the applicability of both methods. We conclude with a simulation study which confirms our findings and show that the k -means algorithm, unlike k -pc, has serious problems in the setting where many pairs in the groups of concomitant extremes exhibit weak asymptotic dependence. Arguably, this is one of the most important settings from the applications point of view (?). In many other cases the results are almost identical, including the 68-dimensional dataset of river discharges and, to a lesser extent, the dietary intake data from [Janssen and Wan \(2020\)](#), which are analysed in Subsection 6.4 and the Supplementary Material, respectively.

2. PRELIMINARIES ON MULTIVARIATE EXTREMES

2.1. The angular distribution. Here we recall some elementary theory of multivariate extremes needed in this paper, and refer the reader to the monograph [Resnick \(2008\)](#) and the surveys of [Davison and Huser \(2015\)](#); [Engelke and Ivanovs \(2021\)](#) for further reading. It is a common practice in extremes to first standardize the marginals and then study extremal dependence. Thus we assume that a random vector $Y \in \mathbb{R}^d$, $d \geq 2$, of interest has unit Fréchet marginal distributions: $\text{pr}(Y_i \leq y) = \exp(-1/y)$ for $y > 0$, $i = 1, \dots, d$. The fundamental regularity assumption on Y , called multivariate regular variation, can be stated as the weak convergence of

the normalized Y conditional on its norm being large:

$$\frac{Y}{\|Y\|_2} \Big| \|Y\|_2 > t \Rightarrow X, \quad t \rightarrow \infty, \quad (1)$$

where the distribution of X is called angular or spectral. This distribution is our main object of interest as it characterizes extremal dependence. It must be noted that any norm can be used here, but we choose the Euclidean norm $\|\cdot\|_2$ so that X lies in $\mathbb{S}_+^{d-1} = \{x \in \mathbb{R}_+^d : \|x\|_2 = 1\}$, which is convenient when considering angular dissimilarities in Section 3. Due to marginal standardization, the mean of X must point to the centre of \mathbb{S}_+^{d-1} :

$$E(X_1) = \dots = E(X_d) = \mu > 0. \quad (2)$$

This property has a certain balancing effect which will come in use later.

The random vector Y satisfying (1) and having unit Fréchet marginals is in the max-domain of attraction of a max-stable distribution uniquely specified by the angle X . It is said that Y admits asymptotic independence (complete dependence) if the limiting max-stable vector has mutually independent (completely dependent) components. The distribution of the corresponding angle X is then as follows:

- (i) *Asymptotic independence*: the distribution of X has mass $1/d$ at every standard basis vector.
- (ii) *Asymptotic complete dependence*: deterministic $X = (1, \dots, 1)/\sqrt{d}$.

A common measure of pairwise asymptotic dependence is the tail dependence coefficient:

$$\chi_{ij} = \lim_{t \rightarrow \infty} \frac{\text{pr}(Y_j > t \mid Y_i > t)}{\text{pr}(Y_i > t)} = \frac{1}{\mu} E(X_i \wedge X_j) \in [0, 1],$$

where 0 corresponds to the asymptotic independence in (i) and 1 to the complete dependence in (ii). These are the boundary cases also in other senses as demonstrated by the following result.

Lemma 2.1. *The constant μ in (2) satisfies $1/d \leq \mu \leq 1/\sqrt{d}$, where the lower bound is achieved iff case (i) holds, and the upper bound is achieved iff case (ii) holds.*

Proof. Note that $\sum_i X_i \geq \|X\|_2 = 1$ and take expectation to get the lower bound. The upper bound follows from $1 = \sum_i E(X_i^2) \geq d\mu^2$. Equality in the latter readily implies that all X_i are constant, whereas equality in the former implies that $X_i X_j = 0$ a.s. for all $i \neq j$. \square

In applications it is common to standardize the observations using the empirical marginal distribution functions and then to choose threshold t large, but such that sufficiently many approximate angles are obtained for the statistical analysis of extremal dependence. This is exactly the procedure used by Janssen and Wan (2020), whose consistency results we will employ in the following. The only difference is that we use unit Fréchet marginals instead of standard Pareto, but these are tail equivalent and no changes in the theory arise.

2.2. Concomitant extremes. In high-dimensional settings it is of crucial importance to identify the non-empty sets of indices $I \subset \{1, \dots, d\}$ such that $\text{pr}(X_i > 0 \ \forall i \in I, X_j = 0 \ \forall j \notin I) > 0$, and the respective probabilities. We will focus on the maximal sets – those not included in other such sets. Let us define the corresponding faces of \mathbb{R}_+^d :

$$F_I = \{x \in \mathbb{R}_+^d : x_j = 0 \ \forall j \notin I\}. \quad (3)$$

According to (2) the probabilities $\text{pr}(X_i > 0)$ are positive for every i , and so every index must be contained in at least one maximal set. The problem at hand is sparse if the cardinality of such sets I is much smaller than d and their number is manageable.

The case (i) of asymptotic independence corresponds to d faces of dimension 1. A more interesting situation occurs when the indices can be partitioned so that asymptotic independence is present between the (disjoint) groups, but not necessarily within these groups. Then any prototype of extremal dependence must belong to some group and, ideally, each group should have a prototype, see Section 4 for further discussion. Thus we arrive to a *basic test scenario*, whereas applicability of the clustering method is much more general:

Assumption A. There exists $2 \leq k \leq d$ and a partition (I_1, \dots, I_k) of the index set $\{1, \dots, d\}$ such that the union of the respective faces F_{I_1}, \dots, F_{I_k} contains the support of the angular measure: $\text{pr}(X \in F_{I_1} \cup \dots \cup F_{I_k}) = 1$. Without loss of generality we assume that the indices in I_i are smaller than those in I_j for all $1 \leq i < j \leq k$.

It may help to also assume that the above partition is unique, but this is not strictly required. The corresponding faces F_{I_1}, \dots, F_{I_k} are mutually orthogonal: $u^\top v = 0$ for all $u \in F_{I_i}, v \in F_{I_j}$ and $i \neq j$, and the only common element is the origin. Even in this scenario identification of the groups of concomitant extremes I_1, \dots, I_k using approximate angles may not be straightforward. For a low-dimensional case of $d = 3$ and the partition $I_1 = \{1, 2\}, I_2 = \{3\}$, Figure 1 depicts a sample from the exact angular law and two samples from its approximations as could arise in practice for different threshold levels t . In these examples both clustering methods produce similar centroids (crosses for k -means and lozenges for k -pc) which are close to the respective faces, and thus the latter can be easily identified.

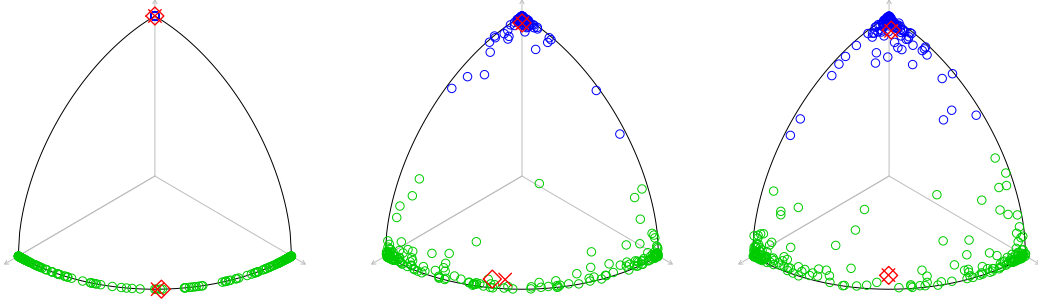


FIGURE 1. A sample of 300 points in \mathbb{S}_+^2 from the exact angular distribution supported by $F_{\{1,2\}} \cup F_{\{3\}}$ and from its approximations. The colours correspond to 2-means / 2-pc clustering with red crosses / lozenges being the centroids.

Let us define the corresponding submodels X_I for $I = I_1, \dots, I_k$ which have the law of the restriction of X to the indices in I conditional on $\{X \in F_I\}$, and let $p_I = \text{pr}(X \in F_I) > 0$ be the respective probabilities. Under Assumption A we thus obtain a complete description of the law of X as a mixture model. Furthermore, $X_I \in \mathbb{S}_+^{|I|-1}$ satisfies (2) with $\mu_I = \mu/p_I$ and so it is a legitimate angular model in dimension $|I|$. Finally, we define the cross-moment matrices

$$\Sigma_I = E(X_I X_I^\top), \quad \Sigma = E(X X^\top) = \text{diag}(p_{I_1} \Sigma_{I_1}, \dots, p_{I_k} \Sigma_{I_k}), \quad (4)$$

where the latter is a block diagonal matrix with $p_I \Sigma_I$ on the diagonal. Note that every Σ_I is a non-negative definite matrix with trace 1, since $\|X_I\|_2 = 1$. An expression of Σ_I for the Hüsler-Reiss distribution is given in Supplementary Material, whereas Remark 3.5 provides connections to the literature on PCA for extremes.

3. SPHERICAL CLUSTERING

3.1. Spherical dissimilarities and Voronoi diagrams. In this section we consider an arbitrary random variable $X \in \mathbb{S}_+^{d-1}$ not necessarily satisfying (2) and return to concomitant extremes in Section 4. Spherical clustering for a given integer $k \geq 1$ amounts to the following stochastic program:

$$\min_{x_1, \dots, x_k \in \mathbb{S}_+^{d-1}} E \left(\min_{i=1}^k c(x_i, X) \right) = 1 - \max_{x_1, \dots, x_k \in \mathbb{S}_+^{d-1}} E \left(\max_{i=1}^k r(x_i^\top X) \right), \quad (5)$$

where $c : \mathbb{S}_+^{d-1} \times \mathbb{S}_+^{d-1} \mapsto [0, 1]$ is a continuous dissimilarity (cost) function. Here we assume that the dissimilarity function has the form $c(x, y) = 1 - r(x^\top y)$ for a strictly increasing continuous (reward) function $r : [0, 1] \mapsto [0, 1]$. In words, the aim is to find k centroids $x_i \in \mathbb{S}_+^{d-1}$ such that the expected dissimilarity of X and the closest centroid is minimal. It is noted that the objective function is continuous in (x_1, \dots, x_k) and the set \mathbb{S}_+^{d-1} is compact, which readily implies that the minimum must be attained. Uniqueness up to a permutation, however, is not guaranteed.

There is a wide choice of popular angular dissimilarity functions used in a variety of contexts (Palarea-Albaladejo et al., 2012), but the above form has an appealing property

$$c(x_1, y) \leq c(x_2, y) \quad \Leftrightarrow \quad x_1^\top y \geq x_2^\top y \quad \Leftrightarrow \quad \|x_1 - y\|_2 \leq \|x_2 - y\|_2,$$

where $x_1, x_2, y \in \mathbb{S}_+^{d-1}$. Thus, for the given k points $x_1, \dots, x_k \in \mathbb{S}_+^{d-1}$ the positive part of the unit sphere will be partitioned into sets A_i by means of hyperplanes in \mathbb{R}^d passing through the origin:

$$A_i = \{y \in \mathbb{S}_+^{d-1} : x_i^\top y \geq x_j^\top y \ \forall j > i, \ x_i^\top y > x_j^\top y \ \forall j < i\}, \quad i = 1, \dots, k. \quad (6)$$

For concreteness, here the equality is broken in favour of the smallest index. Note also that these form the Voronoi diagram of \mathbb{S}_+^{d-1} with respect to the Euclidean norm.

The most popular examples of such cost functions are the scaled Euclidean distance, the angular distance and cosine dissimilarity c_1 , plus we additionally define c_2 corresponding to the quadratic reward function $r(u) = u^2$:

$$\sqrt{1 - x^\top y}, \quad \angle(x, y) = \frac{2}{\pi} \arccos(x^\top y), \quad c_p(x, y) = 1 - (x^\top y)^p, \quad p = 1, 2. \quad (7)$$

The angular distance yields the angle between x and y as the fraction of the right angle $\pi/2$, and such a distance will be useful in numerical experiments below. In clustering one of the most important properties is the simplicity and interpretability of the resulting procedure, and thus we will focus our attention on c_p with $p = 1, 2$. In this case the above clustering problem (5) reduces to maximizing the expected maximal reward $E(\max_i (x_i^\top X)^p)$. For $p = 1$ we retrieve spherical k -means clustering (Dhillon and Modha, 2001), which is intimately related to classical k -means. Finally, $p = 2$ leads to what we call spherical k -pc clustering, which is described below.

Remark 3.1. Importantly, for $p = 2$ we have $r'(0) = 0$, which implies higher cost for two almost orthogonal vectors as compared to the $p = 1$ case. This provides some heuristic support for using the k -pc method instead of k -means in identification of groups of concomitant extremes.

Remark 3.2. While revising this work, we discovered that a similar algorithm had been considered in Hill et al. (2013) under the name ‘perpendicular spherical k -means’. The same cost function is used in this empirical work without observing a link to principal eigenvectors.

3.2. The optimal centroids and partitions. Let us provide some basic results underlying the spherical clustering procedure for the linear and quadratic reward functions. In the first case we will need the normalized means of X restricted to the sets A_i :

$$\bar{x}_i = E(X \mathbf{1}_{\{X \in A_i\}}) / \|E(X \mathbf{1}_{\{X \in A_i\}})\|_2 \in \mathbb{S}_+^{d-1}, \quad (8)$$

where the partition (A_1, \dots, A_k) is given by (6) for an arbitrary choice of $x_1, \dots, x_k \in \mathbb{S}_+^{d-1}$. In order to avoid division by 0 we take $\bar{x}_i = x_i$ when $\text{pr}(X \in A_i) = 0$. In the second case we define $d \times d$ matrices

$$\Sigma_i = E(X X^\top \mathbf{1}_{\{X \in A_i\}}), \quad i = 1, \dots, k. \quad (9)$$

Note the difference between Σ_i and $\Sigma_{\{i\}}$ defined in Section 2. These are non-negative symmetric matrices, which are also non-negative definite. We will be interested in the largest eigenvalue $\lambda_1(\Sigma_i)$ and the corresponding eigenvector \hat{x}_i of Σ_i , assumed to have unit norm: $\|\hat{x}_i\|_2 = 1$. There may be more than one such eigenvector, but at least one of them must have non-negative entries by the Perron–Frobenius theorem, and we choose such. Hence we may assume that $\hat{x}_i \in \mathbb{S}_+^{d-1}$. If the matrix Σ_i is positive or at least irreducible, then such a vector is unique.

The first result forms the basis of the clustering procedure, see (Dhillon and Modha, 2001, Lem. 3.1) for the sample version in the case of the spherical k -means algorithm.

Proposition 3.3. *For $x_1, \dots, x_k \in \mathbb{S}_+^{d-1}$ consider the partition (A_i) in (6). Then*

$$E\left(\max_{i=1}^k x_i^\top X\right) \leq E\left(\max_{i=1}^k \bar{x}_i^\top X\right), \quad E\left(\max_{i=1}^k (x_i^\top X)^2\right) \leq E\left(\max_{i=1}^k (\hat{x}_i^\top X)^2\right),$$

where \bar{x}_i are the normalized means defined in (8) and \hat{x}_i are the normalized principal eigenvectors of the matrices Σ_i defined in (9).

Proof. By definition of A_i and \bar{x}_i we readily obtain

$$E\left(\max_{i=1}^k x_i^\top X\right) = \sum_{i=1}^k x_i^\top E(X \mathbf{1}_{\{X \in A_i\}}) \leq \sum_{i=1}^k \bar{x}_i^\top E(X \mathbf{1}_{\{X \in A_i\}}) \leq E\left(\max_{i=1}^k \bar{x}_i^\top X\right),$$

where the last inequality follows from the fact that only one term among $X \mathbf{1}_{\{X \in A_i\}}$ is non-zero.

By definition of Σ_i we have

$$E\left(\max_{i=1}^k (x_i^\top X)^2\right) = \sum_{i=1}^k E(x_i^\top X \mathbf{1}_{\{X \in A_i\}})^2 = \sum_{i=1}^k x_i^\top \Sigma_i x_i \leq \sum_{i=1}^k \hat{x}_i^\top \Sigma_i \hat{x}_i = \sum_{i=1}^k \lambda_1(\Sigma_i), \quad (10)$$

where we use the standard fact that the quadratic form is maximized under the constraint $\|x\|_2 = 1$ by the principal eigenvector and the maximal value is given by the corresponding eigenvalue, see, e.g., (Overton and Womersley, 1992, Thm. 1). It is left to observe that

$$\sum_{i=1}^k \hat{x}_i^\top \Sigma_i \hat{x}_i = \sum_{i=1}^k E(\hat{x}_i^\top X \mathbf{1}_{\{X \in A_i\}})^2 \leq E\left(\max_{i=1}^k (\hat{x}_i^\top X)^2\right), \quad (11)$$

since only one term among $X \mathbf{1}_{\{X \in A_i\}}$ is non-zero. \square

The above result suggests an iterative procedure for finding the optimal centroids where the updates \bar{x}_i , respectively \hat{x}_i , of the current centroids x_i are used. This procedure will normally converge to a local maximum for the linear, respectively quadratic, reward function. By using a number of different starting centroids we may hope to discover the global maximum and thus solve (5) for the dissimilarity functions c_1 and c_2 . This is exactly the spherical k -means procedure when c_1 and hence the means \bar{x}_i are used.

Importantly, instead of centroids we may optimize over partitions of \mathbb{S}_+^{d-1} :

Corollary 3.4 (Duality). *Let \mathcal{P}_k be the set of partitions of \mathbb{S}_+^{d-1} into k Borel sets. Then*

$$\begin{aligned} \max_{x_1, \dots, x_k \in \mathbb{S}_+^{d-1}} E \left(\max_{i=1}^k x_i^\top X \right) &= \max_{(A_1, \dots, A_k) \in \mathcal{P}_k} \sum_{i=1}^k \|E(X \mathbf{1}_{\{X \in A_i\}})\|_2, \\ \max_{x_1, \dots, x_k \in \mathbb{S}_+^{d-1}} E \left(\max_{i=1}^k (x_i^\top X)^2 \right) &= \max_{(A_1, \dots, A_k) \in \mathcal{P}_k} \sum_{i=1}^k \lambda_1(\Sigma_i), \end{aligned}$$

where Σ_i are defined in (9). Moreover,

- every optimizer (x_1, \dots, x_k) yields an optimal partition (A_1, \dots, A_k) via (6);
- every optimal partition (A_1, \dots, A_k) yields an optimal (x_1, \dots, x_k) given by $x_i = \bar{x}_i$ in the first case and $x_i = \hat{x}_i$ in the second.

Proof. The proof of the two cases is analogous, and we consider only the second case. Let $x_1, \dots, x_k \in \mathbb{S}_+^{d-1}$ be an optimal solution to the left-hand side problem, which exists. By the maximality and (10) we find that the optimal value is $\sum_{i=1}^k \hat{x}_i^\top \Sigma_i \hat{x}_i = \sum_{i=1}^k \lambda_1(\Sigma_i)$. So the supremum over partitions is no smaller. Take an arbitrary partition $(A_1, \dots, A_k) \in \mathcal{P}_k$ with the respective \hat{x}_i and observe that the associated value cannot exceed the maximum over the centroids, see (11). Hence the supremum over the partitions is achieved and the optimal values coincide. \square

Remark 3.5. Matrix Σ has been used by [Cooley and Thibaud \(2019\)](#) and [Drees and Sabourin \(2021\)](#) in their principal component analysis of extremal dependence. Finding the best direction for $X \in \mathbb{S}_+^{d-1}$ corresponds to minimizing the expected c_2 dissimilarity:

$$\min_{x: \|x\|_2=1} E \left(\|X - (x^\top X)x\|_2^2 \right) = 1 - \max_{x: \|x\|_2=1} E(x^\top X)^2 = \min_{x: \|x\|_2=1} E(c_2(x, X)).$$

In the trivial case of $k = 1$ the corresponding centroid $\hat{x}_1 = \lambda_1(\Sigma)$ is the main PCA direction. No such links seem to exist for $k \geq 2$.

3.3. Spherical k -principal-components algorithm. Here we state the algorithm for a discrete distribution putting mass $1/n$ at points $\theta_1, \dots, \theta_n \in \mathbb{S}_+^{d-1}$, not necessarily distinct. Clearly, this setting includes the empirical law. Only a single iteration is described, since the rest is standard. R code is available at https://github.com/jev-ivanovs/spherical_clustering.

Algorithm 3.6. *Spherical k -principal-components clustering – a single iteration.*

Input: the sample $\theta_1, \dots, \theta_n \in \mathbb{S}_+^{d-1}$ and current centroids $x_1, \dots, x_k \in \mathbb{S}_+^{d-1}$.
Compute $n \times k$ matrix of dot products $M = (\theta_1, \dots, \theta_n)^\top (x_1, \dots, x_k)$
Let v be the mean of row-wise maxima of M
For each row of M find the index of the (first) maximal value and store them in g
For $i = 1$ to $i = k$
 Calculate $\Sigma_i = \frac{1}{n} \sum_{u=1}^n (\theta_u \theta_u^\top \mathbf{1}_{\{g_u=i\}})$
 Find the principal eigenvector $\hat{x}_i \in \mathbb{S}_+^{d-1}$ of Σ_i
Output: new centroids $\hat{x}_1, \dots, \hat{x}_k \in \mathbb{S}_+^{d-1}$ and the old value v .

It is easy to see that the running time complexity of this algorithm is $O(k(nd + f(d)))$, where $f(d)$ is the complexity of finding the principal eigenvector of $d \times d$ non-negative symmetric matrix, see [Wang et al. \(2018\)](#) for some basic algorithms and recent developments in this field. Assuming that the spectral gap is bounded away from 0 we may take $f(d) = d^2 \log d$, making k -means and k -pc comparable in the common situation when $d \log d \leq n$.

4. SPHERICAL CLUSTERING AND CONCOMITANT EXTREMES

4.1. Problem formulation. The main goal of this work is to provide some theoretical results supporting clustering for identification of concomitant extremes. The dissimilarities c_1 and c_2 are continuous and hence the consistency result (Janssen and Wan, 2020, Prop. 3.3) readily applies to both types of spherical clustering described above. In words, for high enough threshold t yielding sufficiently many large observations we may expect that clustering of the approximate angles will result in centroids x_1, \dots, x_k close to the true centroids of the angular distribution, given the latter ones are unique up to a permutation. Thus, we may focus on clustering of the exact angular distribution, that is, the distribution of X . The balancing condition (2) will play a crucial role on this way. Some results are still true without this condition and so we stress when it is indeed required.

The basic test scenario is stated in Assumption A, and it gives rise to the following question:

Will spherical clustering of X under Assumption A produce one centroid in each face?

We will see that this is not always the case, and our goal is to identify simple interpretable conditions implying such a result. It turns out that spherical k -pc is preferable to spherical k -means in this setting, since it is more robust and also allows for a substantial theory.

Figure 1 illustrates spherical k -means clustering in the simple case of $d = 3$ and different approximation levels of the angular distribution. Spherical k -pc clustering results in exactly the same assignment of all points (blue/green) to the clusters. The centroids for the two methods are close to each other and also close to the respective faces, and in the case of sampling from the exact law they are, in fact, on the faces $F_{\{1,2\}}$ and $F_{\{3\}}$.

4.2. Fundamental observations. A partial answer to our problem is given by the following characterization result, which readily follows from the clustering duality in Corollary 3.4. The difficult part is in establishing simple sufficient conditions, which we address in Theorem 4.2 and Theorem 5.2. Recall the definition of the submodels X_I in Section 2 and that \mathcal{P}_k is the set of all partitions of \mathbb{S}_+^{d-1} into k Borel sets (or sets of the form (6)).

Proposition 4.1. *Under Assumption A the following is true.*

- k -means: There exist optimal centroids $x_1 \in F_{I_1}, \dots, x_k \in F_{I_k}$ iff

$$\sum_{I=I_1, \dots, I_k} p_I \|E(X_I)\|_2 = \max_{(A_1, \dots, A_k) \in \mathcal{P}_k} \sum_{i=1}^k \|E(X \mathbf{1}_{\{X \in A_i\}})\|_2, \quad (12)$$

where the left-hand side is $\mu(\sqrt{|I_1|} + \dots + \sqrt{|I_k|})$ assuming (2).

- k -pc: There exist optimal centroids $x_1 \in F_{I_1}, \dots, x_k \in F_{I_k}$ iff

$$\sum_{I=I_1, \dots, I_k} p_I \lambda_1(\Sigma_I) = \max_{(A_1, \dots, A_k) \in \mathcal{P}_k} \sum_{i=1}^k \lambda_1(E(X X^\top \mathbf{1}_{\{X \in A_i\}})). \quad (13)$$

Proof. We focus on k -means, since the other result is analogous. Note that the left-hand side of (12) is just $\sum_{i=1}^k \|E(X \mathbf{1}_{\{X \in F_{I_i}\}})\|_2$ and so by Corollary 3.4

$$x_i = E(X \mathbf{1}_{\{X \in F_{I_i}\}}) / \|E(X \mathbf{1}_{\{X \in F_{I_i}\}})\|_2$$

yields an optimal set of centroids, since the given disjoint sets $F_{I_i} \cap \mathbb{S}_+^{d-1}$ can be extended to a partition of \mathbb{S}_+^{d-1} . These indeed satisfy $x_i \in F_{I_i}$.

Next, suppose that some $x_i \in F_{I_i}$ are optimal, and let A_i be the sets in (6), which then yield the maximum. The faces are mutually orthogonal and so every vector $y \in A_i$ in the support of

X also belongs to F_{I_i} , unless $x_i^\top y = 0$ for all i . The latter vectors can be reshuffled between the associated clusters without changing the cost. So we may restrict A_i to F_{I_i} and the first statement follows. Moreover, assuming (2) we have $E(X_I) = \mu_I(1, \dots, 1)^\top$ and so its norm is $\mu_I \sqrt{|I|}$.

In the case of k -pc we also need to observe that the principal eigenvector of $E(XX^\top \mathbf{1}_{\{X \in F_{I_i}\}})$ indeed belongs to F_{I_i} , and the corresponding eigenvalue is $p_{I_i} \lambda_1(\Sigma_{I_i}) > 0$. \square

A simple critical test of any approach is given by the angular distribution corresponding to the asymptotic independence, see case (i) in Section 2. In this case any partition of indices yields faces satisfying Assumption A. We take $k = 2$ for simplicity and partition the index set into $I_1 = \{1, \dots, d_1\}$ and $I_2 = \{d_1 + 1, \dots, d\}$ for some $1 \leq d_1 \leq d - 1$. For k -means the necessary and sufficient condition (12) reads

$$\sqrt{d_1} + \sqrt{d - d_1} = \max_{\ell=0, \dots, d} \{\sqrt{\ell} + \sqrt{d - \ell}\},$$

where ℓ and $d - \ell$ correspond to the alternative partition. But the right-hand side is maximized at $\ell = d/2$ when d is even and $\ell = (d \pm 1)/2$ when d is odd, and so we must choose index sets of essentially equal size to make faces identifiable using k -means, see also Theorem 4.2 below. In the k -pc case we note that $\lambda_1(E(XX^\top \mathbf{1}_{\{X \in A_i\}})) = 1/d$ whenever A_i contains at least one standard basis vector. Thus, the necessary and sufficient condition (13) always holds for such X .

In the above case the partitioning is arbitrary, but one can always construct another angle X' satisfying the moment constraints and arbitrarily close to X such that a given partition becomes the only correct one (the respective faces support the law of X'). This provides a class of examples where k -means clustering fails to identify the supporting faces, because the dissimilarity is continuous, see also Janssen and Wan (2020). Importantly, k -pc does not readily fail in this case.

4.3. Spherical k -means in the size-balanced case. The spherical k -means procedure is guaranteed to identify the correct faces only when their dimensions satisfy a certain strict condition. If this assumption is violated, it is possible to construct a model where k -means fails, see the above discussion.

Theorem 4.2. *Suppose Assumption A and (2) hold. If $d_1 = |I_1|, \dots, d_k = |I_k|$ yield the maximum in*

$$\max_{\substack{d_1, \dots, d_k \in \mathbb{N}_0 \\ d_1 + \dots + d_k = d}} \sqrt{d_1} + \dots + \sqrt{d_k},$$

then there exist optimal centroids (x_1, \dots, x_k) of spherical k -means clustering with $x_i \in F_{I_i}$ for all i . For $k = 2$ this condition reads $||I_1| - |I_2|| \leq 1$.

Proof. In view of (12) it is only required to show that

$$\mu(\sqrt{d_1} + \dots + \sqrt{d_k}) \geq \sum_{i=1}^k \|E(X \mathbf{1}_{\{X \in A_i\}})\|_2$$

for any partition $(A_1, \dots, A_k) \in \mathcal{P}_k$. We denote the right-hand side by $\sum_{i=1}^k \|\nu_i\|_2$ and note that its maximum over $\nu_i \in \mathbb{R}_+^d$ subject to the constraint $\sum \nu_i = E(X) = \mu(1, \dots, 1)^\top$ is attained under the assumption $\nu_i \perp \nu_j$ for all $i \neq j$, see Lemma A.1. Letting δ_i be the number of non-zero entries in ν_i we get an upper bound on the sum of norms:

$$\mu(\sqrt{\delta_1} + \dots + \sqrt{\delta_k}),$$

and the first statement follows. The case $k = 2$ has been discussed above and here the optimal integers d_1, d_2 are such that $|d_1 - d_2| \leq 1$. The proof is complete. \square

5. SPHERICAL k -PRINCIPAL-COMPONENTS CLUSTERING AND CONCOMITANT EXTREMES

5.1. The main result. The eigenvalues of the matrices Σ_I corresponding to the submodels, see Section 2, will play a crucial role in the following. When discussing some basic properties of these matrices we write Σ and assume that $d \geq 1$. Also, let $\lambda_j(M)$ denote the j th largest eigenvalue of a symmetric matrix M , tacitly assuming $\lambda_j(M) = 0$ when j exceeds the order of M . In the case (i) of asymptotic independence Σ is a diagonal matrix with $1/d$ on the diagonal, so that $\lambda_i(\Sigma) = 1/d = \mu$. In the case (ii) of complete dependence Σ is a matrix with constant elements $1/d$ yielding $\lambda_1(\Sigma) = 1, \lambda_2(\Sigma) = 0$. The following lower bound on the largest eigenvalue is true in general.

Lemma 5.1. *Consider $\Sigma = E(XX^\top)$, where $X \in \mathbb{S}_+^{d-1}$ with $d \geq 1$ satisfies (2). Then*

$$\lambda_1(\Sigma) \geq \mu,$$

and the equality implies asymptotic independence.

Proof. Consider the decomposition $\Sigma = \Sigma_0 + \mu^2 \mathbf{1}\mathbf{1}^\top$, where Σ_0 is the respective covariance matrix and $\mathbf{1}$ is a vector of ones. All three matrices are non-negative definite, and the eigenvalues of the latter are $d\mu^2, 0, \dots, 0$. Next, we use the standard inequality: $\lambda_1(\Sigma) \geq \lambda_1(\mu^2 \mathbf{1}\mathbf{1}^\top) = d\mu^2$, which follows from the interpretation of λ_1 as the maximum over quadratic forms, for example. Apply Lemma 2.1 to conclude. \square

We are now ready to state our main result providing some basic theory supporting the use of clustering in detection of groups of concomitant extremes.

Theorem 5.2. *Suppose Assumption A holds. If*

$$\min_{I=I_1, \dots, I_k} p_I \lambda_1(\Sigma_I) \geq \max_{I=I_1, \dots, I_k} p_I \lambda_2(\Sigma_I), \quad (14)$$

then there exist optimal centroids (x_1, \dots, x_k) of spherical k -principal-components clustering such that $x_i \in F_{I_i}$ for all i . Moreover, this condition is satisfied when (2) holds and

$$\lambda_2(\Sigma_I) \leq \mu_I \quad I = I_1, \dots, I_k. \quad (15)$$

Importantly, this sufficient condition asserts that the second principal direction for any face provides a smaller cost reduction than the principal direction of any other face taking the respective probability weights into account. That is, the problem is balanced in this sense. Moreover, the above condition is implied when μ_I separates the first two eigenvalues of Σ_I for all submodels I , see Lemma 5.1. This is true, for example, for certain symmetric models, see Lemma 5.4 below, irrespective of the dimension.

Proof of Theorem 5.2. Let $D_i = p_{I_i} \Sigma_{I_i}$ be the diagonal blocks of Σ . In view of (13), it is only required to show for any partition $(A_1, \dots, A_k) \in \mathcal{P}_k$ that

$$\sum_{i=1}^k \lambda_1(D_i) \geq \sum_{i=1}^k \lambda_1(\Sigma_i),$$

where $\Sigma_i = E(XX^\top \mathbf{1}_{\{X \in A_i\}})$. Lemma A.2 in the Appendix is crucial here, and it shows that the right-hand side is upper bounded by $\sum_{i=1}^k \lambda_i(\Sigma)$. Thus it is left to show that $\sum_{i=1}^k \lambda_1(D_i) \geq \sum_{i=1}^k \lambda_i(\Sigma)$, which is indeed equivalent to the stated assumption, because of the block diagonal structure of $\Sigma = \text{diag}(D_1, \dots, D_k)$.

Now suppose that (2) and (15) are in place. Then $\max_I \{p_I \lambda_2(\Sigma_I)\} \leq \mu \leq \min_I \{p_I \lambda_1(\Sigma_I)\}$, where we apply Lemma 5.1 to each Σ_I . \square

5.2. Simple sufficient conditions. Let us discuss the condition in (15) for a fixed I . Firstly, it is always true for a one- or two-dimensional face, where in the former case we tacitly assume that $\lambda_2 = 0$.

Lemma 5.3. *Assume (2) and $d = 2$. Then $\lambda_2(\Sigma) \leq \mu$.*

Proof. We have $\lambda_1 + \lambda_2 = \text{tr} \Sigma = 1$, and $\lambda_1 \geq \mu$ by Lemma A.2. By Lemma 2.1, $\mu \geq 1/2$, and so $\lambda_2 = 1 - \lambda_1 \leq 1 - \mu \leq \mu$, which completes the proof. \square

Secondly, certain symmetries imply this condition as, for example, invariance of the second moments under permutations.

Lemma 5.4. *Assume (2) and $E(X_i X_j) = E(X_{\pi(i)} X_{\pi(j)})$ for all i, j and all permutations π . Then $\lambda_2(\Sigma) \leq 1/d \leq \mu$.*

Proof. Let $c = E(X_1 X_2) \geq 0$ be the common cross-moment. Observe from $\|X\|_2 = 1$ that $E(X_1^2) = 1/d$, so that Σ is a matrix with diagonal elements $1/d$ and off-diagonal c . It is not difficult to check that $\lambda_1 = 1/d + (d-1)c$ and the other eigenvalues are all equal to $1/d - c$. The proof is complete in view of Lemma 2.1. \square

5.3. Counterexamples. Basic counterexamples to successful identification of faces are obtained by considering more groups of (almost) concomitant extremes than there are clusters. Assume that the index set can be partitioned into 3 sets I_1, I_2, I_3 , but we use $k = 2$ with the partition I_1 and $I_2 \cup I_3$. Write $\Sigma = \text{diag}(D_1, D_2, D_3)$ and suppose that the leading eigenvalues satisfy

$$\lambda_1(D_1) < \lambda_1(D_2) \leq \lambda_1(D_3). \quad (16)$$

Now we readily find that an alternative partition $I_1 \cup I_2$ and I_3 produces a strictly larger value:

$$\lambda_1(D_1) + \lambda_1(\text{diag}(D_2, D_3)) < \lambda_1(\text{diag}(D_1, D_2)) + \lambda_1(D_3),$$

showing that k -pc will fail to identify the faces F_{I_1} and $F_{I_2 \cup I_3}$, see Proposition 4.1 and (4). Of course, the failure is due to the wrong grouping of the three faces, but by continuity of the dissimilarity function we can perturb the model by introducing some small mass on $F_{I_2 \cup I_3}$ without drastically changing the location of the optimal centroids, but making the partition I_1 and $I_2 \cup I_3$ the only possibility.

An example with the property (16) can be produced by taking $|I_1| = 1$ and $|I_2|, |I_3| > 1$ with the latter two submodels being asymptotically dependent, so that $\lambda_1(D_1) = \mu < \lambda_1(D_2) \wedge \lambda_1(D_3)$ according to Lemma 5.1. Examples with $|I_1| > 1$ can be obtained by imposing higher dependence in the subsets I_2 and I_3 .

6. NUMERICAL EXPERIMENTS

6.1. The simulation framework. Firstly, we consider a $d = 100$ dimensional model satisfying Assumption A with $k = 2$ faces. The k -means and k -pc algorithms are compared by attempting to associate each pair of centroids with the two faces and computing certain scores. Secondly, we consider a more practical situation where the groups are not disjoint and the number of groups k must be inferred from data. Finally, we apply both clustering algorithms to two real world datasets.

Here we briefly describe our basic model used in simulations. The random vector Y is taken to have a d -variate max-stable Hüsler–Reiss distribution introduced in [Hüsler and Reiss \(1989\)](#) and further studied in [Engelke et al. \(2015\)](#); [Engelke and Hitz \(2020\)](#). This popular family has a good control of pairwise extremal dependencies which are encoded into the associated variogram matrix Γ parametrizing the distribution. The variogram satisfying Assumption [A](#) with $k = 2$ faces of dimensions d_1 and d_2 is produced randomly in a certain way detailed in the Supplementary Material. The pairwise tail dependence coefficients are likely to be very small in our parameter generation procedure. This may lead to a subdivision of a group of concomitant extremes into almost independent subgroups making the detection problem harder, see Section [4](#).

In each experiment we sample 10^4 i.i.d. realizations of Y using the R package [Engelke et al. \(2019\)](#). We take 10% of these vectors having the largest Euclidean norm and thus form 10^3 approximate realizations of the angle X . An example of the estimated matrix (χ_{ij}) appears in Figure [3](#) (left). The mean is 0.21 for asymptotically dependent $i \neq j$ and 0.1 for the pairs with asymptotic independence.

One way to obtain faces from the centroids $x \in \mathbb{S}_+^{d-1}$ is to use a simple truncation procedure: $I = \{i : x_i > \delta\}$ for a chosen level $\delta > 0$. Another way is to find the index set I with the minimal cardinality and such that the angle with the respective face is sufficiently small: $\angle(x, F_I) < \varepsilon$, where

$$\angle(x, F_I) = \min\{\angle(x, y) : y \in F_I \cap \mathbb{S}_+^{d-1}\} = \frac{2}{\pi} \arccos \left[\left(\sum_{i \in I} x_i^2 \right)^{1/2} \right] \in [0, 1], \quad (17)$$

see also [\(7\)](#). The last equality follows from the fact that the minimizer y is given by the normalized vector $(x_i \mathbf{1}_{\{i \in I\}})_{i=1}^d$. Finding such I is simple, since we only need to choose enough indices corresponding to the largest x_i 's. Note that by doing so we always pick a face yielding the smallest angle with x among all faces of the same dimension. This latter approach is more consistent with the spherical clustering paradigm, and so we use it throughout our experiments. In fact, any dissimilarity in Section [3](#) would produce the same results up to changing the threshold appropriately.

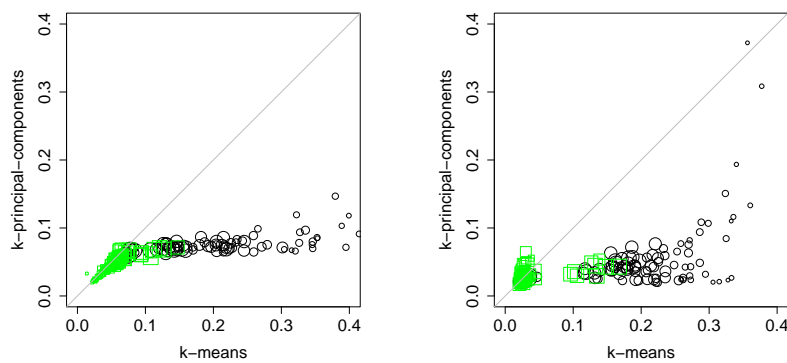


FIGURE 2. Left: angles to the corresponding faces. Right: maximal entries over I^c . Black circles correspond to the first face, green squares to the second, and scale to d_1 .

6.2. Comparison of k -means and k -pc. We replicate the following procedure 100 times: we choose $d_1 \in \{1, \dots, 50\}$ uniformly at random and generate a variogram Γ corresponding to the partition $I_1 = \{1, \dots, d_1\}$ and $I_2 = \{d_1 + 1, \dots, 100\}$. Then we produce 10^3 approximate

realizations of the angle X , apply both the k -means and k -pc algorithms using $k = 2$ and 100 random restarts in each, and associate each pair of centroids with the two faces. For each centroid x we calculate the angle to the corresponding face $\angle(x, F_I)$ defined in (17) and the maximal entry $\max\{x_i : i \in I^c\}$ over the indices defining the other face. That is, a small number indicates that the centroid is indeed close to its face, see Figure 2 where 19 and 8 black points are outside the plot range, respectively.

We call it an error when a centroid yields the angle and the maximal entry both exceeding 0.1. Out of 200 trials (faces) there are approximately 46% errors for k -means and only 8% for k -pc, and all of the latter are also the errors for the k -means procedure. By increasing the threshold to 0.2 we get 26% and 5% of errors, and again all the errors in the latter are also errors in the former. Furthermore, these correspond to the first face and occur when it is relatively small. We also check that in all these cases permuting the assignment to faces does not resolve the issue.

In the above regime of weak asymptotic dependence the k -pc method outperforms k -means, which is also expected in view of the above developed theory and accompanying intuition. In the case of increased dependence within the faces both clustering methods perform extremely well, making identification of the corresponding faces an obvious task in this simplistic setting.

6.3. Non-orthogonal faces and the choice of k . Recall that Assumption A is required for our theoretical guarantees alone. Here we consider a typical scenario where the groups of concomitant extremes have common elements and the number of groups k must be inferred from data. We mix two datasets: half of the observations come from the above (randomly sampled) Hüsler–Reiss model with two groups $\{1, \dots, 40\}, \{61, \dots, 100\}$ and half from an analogous model with two groups $\{21, \dots, 60\}, \{1, \dots, 20, 61, \dots, 100\}$. These are the underlying four faces to be identified. The estimated matrix of tail dependence coefficients (χ_{ij}) is presented in Figure 3 (left). This image may give a false feeling that identification of groups is easy, and so we reorder the indices according to the standard heatmap routine in R based on hierarchical clustering, see Figure 3 (centre). Now the groups cannot be easily seen with a naked eye.

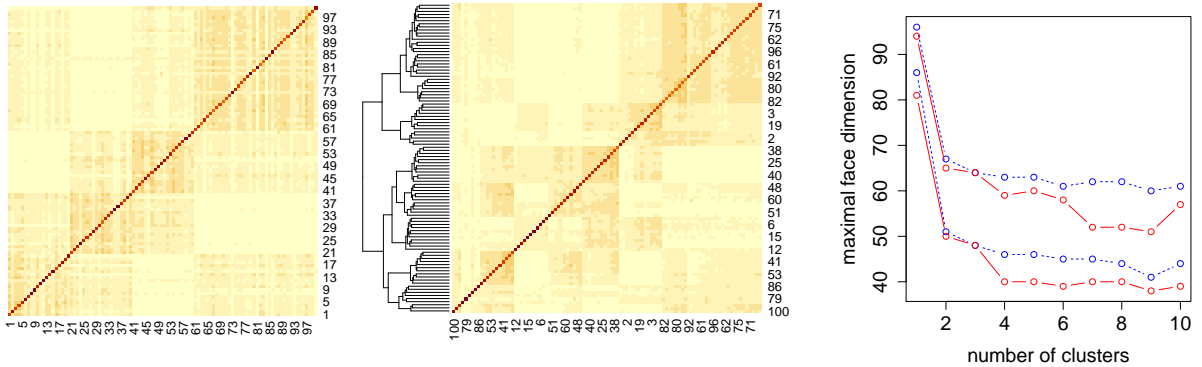


FIGURE 3. Non-orthogonal faces: estimated (χ_{ij}) , its heatmap, and maximal face dimension for $\varepsilon \in \{1/10, 1/5\}$ with k -pc in solid red.

We run k -means and k -pc for $k = 1, \dots, 10$ and use 500 restarts in each (much fewer would be sufficient for smaller k). The standard ‘elbow plot’ of the cost as a function of k does not reveal a clear candidate for the number of clusters, and so is omitted. Importantly, our final goal is not to cluster the points but rather to determine the groups of concomitant extremes, hopefully leading to a sparse model. Thus, instead of plotting the cost function, we plot the maximal face dimension in Figure 3 (right) for two (angular) thresholds $\varepsilon \in \{1/10, 1/5\}$, which does suggest

$k = 4$ as an adequate candidate when using k -pc (in red). Choosing the right k is difficult in general, and one may look at various statistics depending on the problem and goals of the study. Providing some theory to aid this choice is an important open question.

Finally, we present the detected 4 faces in Figure 4, where the same two thresholds are used. Note that smaller threshold leads to larger faces and we depict additional indices by light colors. Here and below the thresholds are chosen so that the recovered faces correspond to a sparse problem while (almost) all indices are contained in some group. In Figure 4, the centroids are ordered so that the respective faces can be associated with $\{1, \dots, 40\}$, $\{21, \dots, 60\}$, $\{1, \dots, 20, 61, \dots, 100\}$ and $\{41, \dots, 100\}$. Both methods produce relatively good results with k -pc being visually a bit better. Choosing an appropriate threshold is non-trivial and this choice may depend on the ability to cope with faces of large dimension in a subsequent modelling step. Larger threshold values result in smaller faces. Some indices may not appear in any group indicating their high level of asymptotic independence from the rest. In practice, it may be reasonable to first establish the main directions/prototypes of extremes and then treat the remaining components in some way. Finally, thresholding of centroids is just one possibility to define faces, and many others exist (Chautru, 2015).

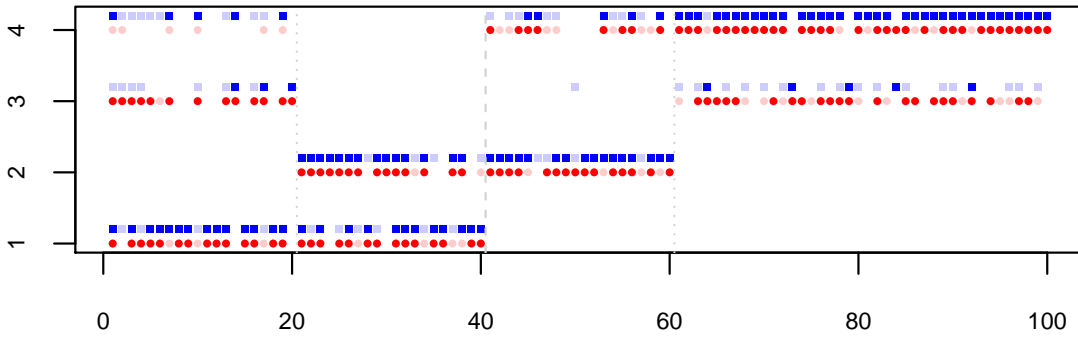


FIGURE 4. Detection of 4 non-orthogonal faces using k -means (blue) and k -pc (red) with $\varepsilon = 1/5$ (dark colours) and $\varepsilon = 1/10$ (both intensities).

6.4. River discharges. We illustrate the two clustering approaches using river discharges at $d = 68$ locations in Switzerland, see the review paper Engelke and Ivanovs (2021) for a detailed description of this dataset. The data is standardized as described in Section 2 and then 10% of observations are used to approximate the angular distribution, resulting in 202 samples. Unlike in the simulation experiments above, here we have a rather strong ‘asymptotic’ dependence between various components, see Figure 5 (left).

First, we investigate a basic thresholding approach without clustering as in the DAMEX algorithm (Goix et al., 2016), which assigns extreme observations (with respect to the max norm) to faces according to a chosen threshold. Figure 5 (centre) presents some statistics for various thresholds and also illustrates a common issue with this approach, see also Goix et al. (2017) and Chiapino et al. (2020) for further comments and possible solutions. This method results in a large number of faces with a single observation, and so further grouping is needed. Note that pruning such faces would remove a majority of the extreme observations. Upon reducing the threshold, we get one high-dimensional face containing most of the observations. In the above example of 4 non-orthogonal faces an analogous picture is obtained. Furthermore, similar issues

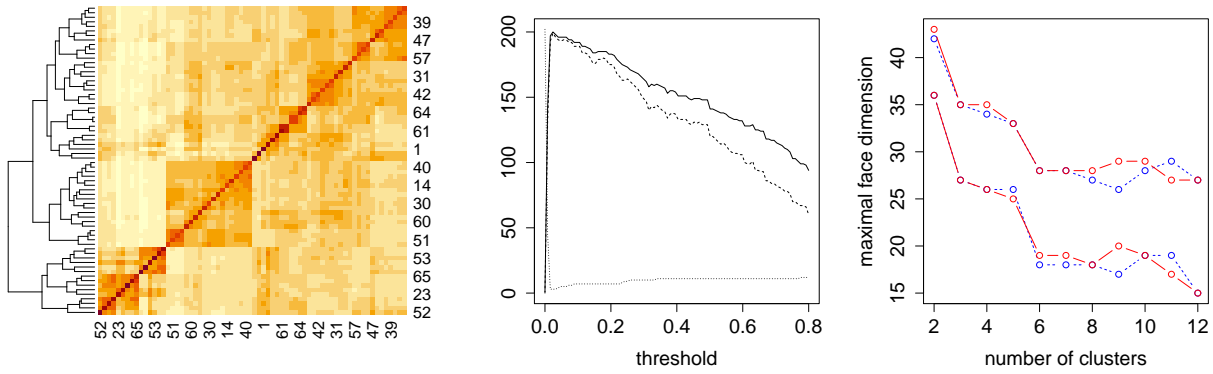


FIGURE 5. Left: estimated (χ_{ij}) . Centre: truncation without clustering – # faces (solid), # faces with a single observation (dashed), max # observations per face (dotted). Right: clustering – max face dimension for $\varepsilon \in \{1/4, 1/3\}$.

(even if less pronounced) arise when using the alternative approach of [Meyer and Wintenberger \(2021\)](#) in this and the previous examples.

Next, we consider clustering approaches with a relatively small number of clusters $k = 2, \dots, 12$, which is desirable in practice, since every cluster leads to a submodel requiring further investigation. In all cases the centroids produced by the two methods are very similar with the maximal angular distance of 0.1; here we used 30000 restarts to limit the effect of sub-optimal centroids. Figure 5 (right) illustrates the maximal face dimension as a function of k , which suggests $k = 6$ as an adequate number of faces. The obtained faces using $\varepsilon = 1/4$ are depicted in Figure 6, see also [Engelke and Ivanovs \(2021\)](#) for a somewhat similar picture. These groups of concomitant extremes exhibit nice geographical patterns. The face dimensions are 27, 15, 4, 8, 28, 11 (from smaller to larger circles) containing 46, 41, 19, 35, 38, 23 extreme observations, respectively. It is noted that the k -means centroids are almost the same, the cluster assignments of observations coincide, and the faces differ only slightly. A more careful analysis may proceed by using different thresholds for each centroid, or some other face attribution procedure.

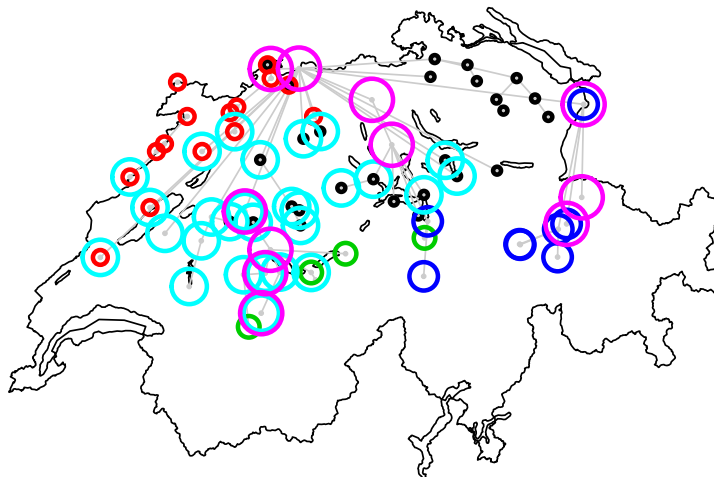


FIGURE 6. River network with 68 gauging stations denoted by gray points. The $k = 6$ faces obtained using the k -pc method are depicted using circles of different color and size.

In conclusion, the spherical clustering approach is a useful tool in the analysis of concomitant extremes in large dimensions. The two methods often produce similar results, but the k -pc method may be better in the setting when the groups exhibit weak asymptotic dependence between many pairs of their components. Importantly, it comes with a theoretical guarantee applicable in a much broader context, which is the main contribution of this work.

ACKNOWLEDGEMENT

The authors gratefully acknowledge financial support of Sapere Aude Starting Grant 8049-00021B “Distributional Robustness in Assessment of Extreme Risk”.

APPENDIX A. TWO LEMMAS

The first result is required for the proof of Theorem 4.2.

Lemma A.1. *A maximizer (ν_1, \dots, ν_k) of*

$$\max_{\nu_1, \dots, \nu_k \in \mathbb{R}_+^d} \sum_{i=1}^k \|\nu_i\|_2 \quad \text{subject to} \quad \sum_{i=1}^k \nu_i = \nu \in \mathbb{R}_+^d$$

satisfies for all $i \neq j$: $\nu_i \perp \nu_j$ or both ν_i and ν_j have one positive entry at the same position. Moreover, if $k \leq d$, then the maximum is attained under the assumption $\nu_i \perp \nu_j$ for all $i \neq j$.

Proof. The maximum is attained since it is the maximum of a continuous function over a compact set. Assume that for some index ℓ we have $a = \nu_{i\ell} > 0$ and $b = \nu_{j\ell} > 0$, which is equivalent to $\nu_i \perp \nu_j$. Let $c = (\sum_{m \neq \ell} \nu_{im}^2)^{1/2} \geq 0$ and $d = (\sum_{m \neq \ell} \nu_{jm}^2)^{1/2} \geq 0$ be the norms when the ℓ th coordinate is ignored. We further assume that $c + d > 0$, which excludes the possibility of only one positive entry. It is enough to show that there exists a vector $u \in \mathbb{R}^d$ such that

$$\|\nu_i + u\|_2 + \|\nu_j - u\|_2 > \|\nu_i\|_2 + \|\nu_j\|_2, \quad \nu_i + u, \nu_j - u \geq 0,$$

so that the maximality fails. We will consider the two possibilities $u = be_\ell$ and $u = -ae_\ell$, where e_ℓ is the ℓ th standard basis vector. It is clear that the positivity constraint is satisfied. Thus it is enough to show that

$$\max\{\sqrt{(a+b)^2 + c^2} + d, c + \sqrt{(a+b)^2 + d^2}\} > \sqrt{a^2 + c^2} + \sqrt{b^2 + d^2}, \quad (18)$$

where $a, b > 0$, $c, d \geq 0$ and $c + d > 0$, which can be proved by assuming that $d > c$ so that the first entry in the maximum is larger than the second, and taking squares of both sides twice.

Finally, any group of ν_i with a single strictly positive entry in the same position can be replaced by their sum and zero vectors without changing the sum of norms. \square

The proof of Theorem 5.2 relies on the following non-standard upper bound on the sum of leading eigenvalues.

Lemma A.2. *Let M_1, \dots, M_k be symmetric non-negative definite matrices of order $d \geq k$. Then*

$$\sum_{i=1}^k \lambda_1(M_i) \leq \sum_{i=1}^k \lambda_i(M), \quad M = \sum_{i=1}^k M_i. \quad (19)$$

Moreover, for any M there exist M_i as above yielding the equality.

Proof. By the result of [Fan \(1949\)](#), see also ([Overton and Womersley, 1992](#), Thm. 1), we have

$$\sum_{i=1}^k \lambda_i(M) = \max \left\{ \sum_{i=1}^k v_i^\top M v_i : v_i^\top v_j = 1_{\{i=j\}} \right\} \quad (20)$$

and, in particular, $\lambda_1(M) = \max\{v^\top M v : \|v\|_2 = 1\}$.

Let vectors u_1, \dots, u_k have unit norms and be such that $\lambda_1(M_i) = u_i^\top M_i u_i$, and let v_1, \dots, v_k be mutually orthogonal vectors with unit norms obtained via the Gram–Schmidt process. That is, for all $i = 1, \dots, k$ we have $u_i = \sum_{j=1}^i c_{ij} v_j$, where $\sum_{j=1}^i c_{ij}^2 = 1$.

By (20) we have

$$\sum_{j=1}^k \lambda_j(M) \geq \sum_{j=1}^k v_j^\top M v_j = \sum_{i=1}^k \sum_{j=1}^k v_j^\top M_i v_j \geq \sum_{i=1}^k \sum_{j=1}^i v_j^\top M_i v_j,$$

where in the last step we use the assumption that M_i are non-negative definite. Furthermore, for any i we have the representation

$$\lambda_1(M_i) = u_i^\top M_i u_i = \left(\sum_{j=1}^i c_{ij} v_j^\top \right) M_i \left(\sum_{j=1}^i c_{ij} v_j \right) = \sum_{j=1}^i c_{ij}^2 v_j^\top M_i v_j + \sum_{j \leq i} \sum_{j \neq \ell \leq i} c_{ij} c_{i\ell} v_j^\top M_i v_\ell.$$

Thus, we find a lower bound on the difference of interest:

$$\sum_{i=1}^k \lambda_i(M) - \sum_{i=1}^k \lambda_1(M_i) \geq \sum_{i=1}^k \left(\sum_{j=1}^i (1 - c_{ij}^2) v_j^\top M_i v_j - \sum_{j \leq i} \sum_{j \neq \ell \leq i} c_{ij} c_{i\ell} v_j^\top M_i v_\ell \right).$$

But according to the constraints on c_{ij} we have

$$\sum_{j=1}^i (1 - c_{ij}^2) v_j^\top M_i v_j = \sum_{j \leq i} \sum_{j \neq \ell \leq i} c_{i\ell}^2 v_j^\top M_i v_j,$$

and it is left to check non-negativity of the terms

$$\sum_{j \leq i} \sum_{j \neq \ell \leq i} (c_{i\ell}^2 v_j^\top M_i v_j - c_{ij} c_{i\ell} v_j^\top M_i v_\ell) = \sum_{1 \leq \ell < j \leq i} (c_{i\ell} v_j - c_{ij} v_\ell)^\top M_i (c_{i\ell} v_j - c_{ij} v_\ell),$$

which is true due to assumed non-negative definiteness of all M_i , and the first assertion is proven.

The second assertion is obtained by taking the matrices

$$\begin{aligned} M_i &= Q \text{diag}(0, \dots, 0, \lambda_i(M), 0, \dots, 0) Q^\top, \quad 1 \leq i \leq k-1, \\ M_k &= Q \text{diag}(0, \dots, 0, \lambda_k(M), \lambda_{k+1}(M), \dots, \lambda_d(M)) Q^\top, \end{aligned}$$

where Q is an orthogonal matrix in the diagonalization of M . Indeed, the matrices M_i are non-negative definite summing up to M , and the largest eigenvalues are $\lambda_i(M)$ for $i \leq k$. \square

APPENDIX B. HÜSLER–REISS DISTRIBUTION

B.1. Random generation of variogram. A d -dimensional max-stable Hüsler–Reiss distribution ([Hüsler and Reiss, 1989](#)) is parametrized by a conditionally negative definite $d \times d$ matrix Γ , called a variogram. Every such matrix has a representation $\Gamma_{ij} = \|h_i - h_j\|_2^2$, where h_1, \dots, h_d are the elements of some Hilbert space with norm $\|\cdot\|_2$, and every such construction yields a conditionally negative definite matrix, see ([Vakhania et al., 1980](#), Property (g), p. 191). As usual, we impose a further non-degeneracy assumption that Γ is strictly conditionally negative definite so that the associated exponent measure has a density ([Engelke et al., 2015](#)).

Suppose that Y has a max-stable Hüsler–Reiss distribution. Our main assumption requires a partition $I_1 \cup I_2 = \{1, \dots, d\}$ of the index set such that $\chi_{ij} = \chi_{ji} = 0$ for all $i \in I_1$ and $j \in I_2$,

which is equivalent to (asymptotic) independence of the two groups of components of Y . Recall the formula for the bivariate tail dependence coefficient:

$$\chi_{ij} = 2\bar{\Phi}(\sqrt{\Gamma_{ij}}/2),$$

where $\bar{\Phi}$ is the survival function of the standard normal distribution, and note that $\chi_{ij} = 0$ is obtained in the limit case $\Gamma_{ij} = \infty$. In practice, large entries in the respective locations of Γ would suffice, because of the weak convergence of the respective distributions.

In our experiments we randomly generate Γ for $d = 100$ according to the following procedure based on the aforementioned representation. Firstly, we generate d -dimensional vectors h_1, \dots, h_d with i.i.d. Pareto distributed components having shape parameter 2.5. Secondly, we add one more dimension by letting $\tilde{h}_i = (h_i, L\mathbf{1}_{\{i \in I_1\}})$, where $L = 10^5$ is a fixed large number. Then the variogram matrix Γ is set to $\frac{3}{d}(\|\tilde{h}_i - \tilde{h}_j\|_2^2)_{ij}$, where $3/d$ provides a scaling resulting in a suitable distribution of the tail dependence coefficients. Note that this procedure ensures that $\Gamma_{ij} \geq L$ for i and j in different groups.

Finally, we use the R package (Engelke et al., 2019) to sample vectors Y from the Hüsler–Reiss distribution specified by Γ . Note that $Y/\|Y\|_2$ given $\|Y\|_2 > t$ for a finite threshold t provides only an approximation of the limiting angle. The distribution of the exact angle is addressed below.

B.2. The angular distribution and the matrix Σ . Even though the exact matrix $\Sigma = E(XX^\top)$ is not required for the simulation experiments, it can be used to verify the sufficient conditions in our main result. Below we determine the probability density function of X (with respect to the Euclidean norm) and provide an expression for Σ in terms of expectations of transformed Gaussian vectors.

As in Engelke et al. (2015), we consider the $(d-1) \times (d-1)$ covariance matrix

$$R = \left\{ \frac{1}{2}(\Gamma_{id} + \Gamma_{jd} - \Gamma_{ij}) \right\}_{i,j \neq d}.$$

For all $i = 1, \dots, d$ we define the transformation

$$t_i(x) = \log(x_i/x_d) = \log\left(x_i/\sqrt{1 - x_1^2 - \dots - x_{d-1}^2}\right), \quad x \in \text{int}(\mathbb{S}_+^{d-1}), \quad (21)$$

where $\text{int}(\mathbb{S}_+^{d-1})$ stands for the simplex interior, and note that $t: \text{int}(\mathbb{S}_+^{d-1}) \rightarrow \mathbb{R}^{d-1}$ is a bijection with the inverse

$$t^{-1}(z) = \frac{(\exp(z_1), \dots, \exp(z_{d-1}), 1)^\top}{\sqrt{1 + \exp(2z_1) + \dots + \exp(2z_{d-1})}}.$$

It turns out that each column of the matrix Σ/μ corresponds (up to a permutation) to $E(t^{-1}(Z))$ for a multivariate normal Z as specified below. The means and other moments of X can be obtained in a similar way.

Lemma B.1. *For the d -dimensional Hüsler–Reiss distribution with the variogram Γ the density of the Euclidean angle (X_1, \dots, X_{d-1}) is given by*

$$f(x_1, \dots, x_{d-1}) = \mu x_d^{-2} \prod_{i \leq d} x_i^{-1} \phi_{d-1}(t_1(x), \dots, t_{d-1}(x)), \quad x \in \text{int}(\mathbb{S}_+^{d-1}), \quad (22)$$

where $\mu = E(X_1)$ and ϕ_{d-1} is the density of the multivariate normal distribution with covariance matrix R and mean vector $-(\Gamma_{1d}, \dots, \Gamma_{d-1,d})^\top/2$. Furthermore, with g being the density of

(W_1, \dots, W_{d-1}) , where $W = t^{-1}(Z) \in \mathbb{S}_+^{d-1}$ and $Z \sim \phi_{d-1}$, the following identities hold:

$$f(x_1, \dots, x_{d-1}) = \mu g(x_1, \dots, x_{d-1})/x_d, \\ \mu^{-1} = E(W_d^{-1}), \quad E(X_i X_d) = \mu E(W_i), \quad i = 1, \dots, d.$$

Proof. From [Engelke et al. \(2015\)](#) it is known that the exponent measure has the density

$$\lambda(y) = y_d^{-1} \prod_{i \leq d} y_i^{-1} \phi_{d-1}(\log(y_1/y_d), \dots, \log(y_{d-1}/y_d)), \quad y_1, \dots, y_d > 0.$$

We note that for the polar coordinates

$$y_1 = r x_1, \quad y_2 = r x_2, \quad \dots, \quad y_d = r(1 - x_1^2 - \dots - x_{d-1}^2)^{1/2}$$

the absolute value of the Jacobian evaluates to r^{d-1}/x_d , and so in these coordinates the density becomes

$$r^{-2} x_d^{-2} \prod_{i \leq d} x_i^{-1} \phi_{d-1}(t_1(x), \dots, t_{d-1}(x)).$$

This must factorize into $r^{-2} f(x_1, \dots, x_{d-1})/\mu$ according to ([Resnick, 2008](#), Prop. 5.11(iv)) and the first result follows.

Let us compute the Jacobian $J_t(x)$ of the transformation $t(x)$ defined in (21) and restricted to the first $d-1$ values. We have

$$\frac{\partial t_i}{\partial x_j}(x) = \frac{x_j}{s}, \quad j \neq i, \quad \text{and} \quad \frac{\partial t_i}{\partial x_i}(x) = \frac{x_i^2 + s}{x_i s},$$

where $s = 1 - x_1^2 - \dots - x_{d-1}^2 = x_d^2$, and so

$$J_t(x) = \begin{vmatrix} \frac{x_1^2 + s}{x_1 s} & \frac{x_2}{x_1 s} & \dots & \frac{x_{d-1}}{x_1 s} \\ \frac{x_1}{x_2 s} & \frac{x_2^2 + s}{x_2 s} & \dots & \frac{x_{d-1}}{x_2 s} \\ \vdots & \vdots & \ddots & \vdots \\ \frac{x_1}{x_{d-1} s} & \frac{x_2}{x_{d-1} s} & \dots & \frac{x_{d-1}^2 + s}{x_{d-1} s} \end{vmatrix} = \frac{x_1 \dots x_{d-1}}{s^{d-1}} \begin{vmatrix} \frac{s}{x_1^2} + 1 & 1 & \dots & 1 \\ 1 & \frac{s}{x_2^2} + 1 & \dots & 1 \\ \vdots & \vdots & \ddots & \vdots \\ 1 & 1 & \dots & \frac{s}{x_{d-1}^2} + 1 \end{vmatrix}.$$

Using formula (1) in [Goberstein \(1980\)](#), we find that the last determinant is equal to

$$\frac{s^{d-1}}{x_1 \dots x_{d-1}} + \frac{s^{d-1}}{x_1 \dots x_{d-1}} \cdot \left(\frac{x_1^2}{s} + \dots + \frac{x_{d-1}^2}{s} \right) = \frac{1}{x_1 \dots x_{d-1} s}.$$

Thus, we have the relation $g(x) = (x_1 \dots x_{d-1} s)^{-1} \phi_{d-1}(t(x))$, where x and $t(x)$ are restricted to the first $d-1$ elements. Comparing it with f , we indeed find the stated relation between f and g . Finally, observe that

$$E(X_i X_d) = \mu \int x_i g(x) dx = \mu E(W_i), \quad 1 = \mu E(W_d^{-1}).$$

The proof is complete. \square

The above result states that the last column of Σ/μ is given by the vector $E(W)$. By changing the indexing we may easily find the other columns. In particular, in the bivariate case with parameter $\gamma = \Gamma_{12}$ we have

$$W_1 = [1 + \exp(-2\sqrt{\gamma}Z_0 + \gamma))]^{-1/2}, \quad W_2 = (1 - W_1^2)^{1/2} = [1 + \exp(2\sqrt{\gamma}Z_0 - \gamma))]^{-1/2},$$

where Z_0 is a standard normal. Sadly, the moments $w_1 = E(W_1)$, $w_2 = E(W_2)$ are not explicit, and the same applies to the matrix $\Sigma/\mu = \begin{pmatrix} 1-w_2 & w_1 \\ w_1 & w_2 \end{pmatrix}$.

REFERENCES

- Chautru, E. (2015). Dimension reduction in multivariate extreme value analysis. *Electron. J. Stat.*, 9(1):383–418.
- Chiapino, M., Cl  men  on, S., Feuillard, V., and Sabourin, A. (2020). A multivariate extreme value theory approach to anomaly clustering and visualization. *Computational Statistics*, 35:607–628.
- Cooley, D. and Thibaud, E. (2019). Decompositions of dependence for high-dimensional extremes. *Biometrika*, 106(3):587–604.
- Davison, A. and Huser, R. (2015). Statistics of extremes. *Ann. Rev. Stat. App.*, 2:203–235.
- Dhillon, I. S. and Modha, D. S. (2001). Concept decompositions for large sparse text data using clustering. *Machine learning*, 42(1-2):143–175.
- Drees, H. and Sabourin, A. (2021). Principal component analysis for multivariate extremes. *Electron. J. Statist.*, 15(1):908–943.
- Engelke, S. and Hitz, A. S. (2020). Graphical models for extremes. *J. R. Stat. Soc. B.*, 82(4):871–932.
- Engelke, S., Hitz, A. S., and Gnecco, N. (2019). *graphicalExtremes: Statistical Methodology for Graphical Extreme Value Models*. Available from <https://CRAN.R-project.org/package=graphicalExtremes>, R package version 0.1.0.
- Engelke, S. and Ivanovs, J. (2021). Sparse structures for multivariate extremes. *Annu. Rev. Stat. Appl.*, 8(1):241–270.
- Engelke, S., Malinowski, A., Kabluchko, Z., and Schlather, M. (2015). Estimation of H  sler–Reiss distributions and Brown–Resnick processes. *J. R. Stat. Soc. B.*, 77(1):239–265.
- Fan, K. (1949). On a theorem of Weyl concerning eigenvalues of linear transformations I. *Proceedings of the NAS of the USA*, 35(11):652.
- Gan, G., Ma, C., and Wu, J. (2007). *Data clustering*, volume 20. SIAM and ASA. Theory, algorithms, and applications.
- Goberstein, S. M. (1980). Evaluating ”uniformly filled” determinants. *Col. Math. J.*, 19(4):343–345.
- Goix, N., Sabourin, A., and Cl  men  on, S. (2016). Sparse representation of multivariate extremes with applications to anomaly ranking. In *Proceedings of the 19th International Conference on Artificial Intelligence and Statistics (AISTATS)*. JMLR: W&CP.
- Goix, N., Sabourin, A., and Cl  men  on, S. (2017). Sparse representation of multivariate extremes with applications to anomaly detection. *J. Multivar. Anal.*, 161:12–31.
- Hill, M. O., Harrower, C. A., and Preston, C. D. (2013). Spherical k -means clustering is good for interpreting multivariate species occurrence data. *Methods Ecol. Evol.*, 4(6):542–551.
- H  sler, J. and Reiss, R.-D. (1989). Maxima of normal random vectors: between independence and complete dependence. *Stat. Prob. Let.*, 7(4):283–286.
- Jalalzai, H. and Leluc, R. (2020). Informative clusters for multivariate extremes. *arXiv:2008.07365*.
- Janssen, A. and Wan, P. (2020). k -means clustering of extremes. *Electron. J. Stat.*, 14:1211–1233.
- Larsson, M. and Resnick, S. I. (2012). Extremal dependence measure and extremogram: the regularly varying case. *Extremes*, 15:231–256.
- Meyer, N. and Wintenberger, O. (2021). Sparse regular variation. *Advances in Applied Probability*, 53(4):1115–1148.

- Overton, M. L. and Womersley, R. S. (1992). On the sum of the largest eigenvalues of a symmetric matrix. *SIMAX*, 13(1):41–45.
- Palarea-Albaladejo, J., Martín-Fernández, J. A., and Soto, J. A. (2012). Dealing with distances and transformations for fuzzy c -means clustering of compositional data. *J. Classif.*, 29(2):144–169.
- Resnick, S. I. (2008). *Extreme Values, Regular Variation and Point Processes*. Springer, New York.
- Simpson, E. S., Wadsworth, J. L., and Tawn, J. A. (2020). Determining the dependence structure of multivariate extremes. *Biometrika*, 107(3):513–532.
- Vakhania, N. N., Tarieladze, V. I., and Chobanyan, S. A. (1980). *Probability Distributions on Banach Spaces*. Mathematics and Its Applications (Soviet Series). D. Reidel Publishing Company.
- Wang, J., Wang, W., Garber, D., and Srebro, N. (2018). Efficient coordinate-wise leading eigenvector computation. In *Algorithmic Learning Theory*, pages 806–820. PMLR.

AARHUS UNIVERSITY, DEPARTMENT OF MATHEMATICS, DENMARK